

Influence of electronic correlations on the frequency-dependent hopping transport in Si:P

Elvira Ritz and Martin Dressel

1. Physikalisches Institut, Universität Stuttgart, Pfaffenwaldring 57, 70550 Stuttgart, Germany

Received 6 August 2007, revised 17 September 2007, accepted 18 September 2007

Published online 7 February 2008

PACS numbers: 71.30.+h, 72.15.Rn, 72.20.Ee, 72.80.Ng

Corresponding author: e-mail ritz@pi1.physik.uni-stuttgart.de, Phone +49-(0)711-68564893, Fax +49-(0)711-68564886

At low energy scales charge transport in the insulating Si:P is dominated by activated hopping between the localized donor electron states. Thus, theoretical models for a disordered system with electron-electron interaction are appropriate to interpret the electric conductivity spectra. With a newly developed technique we have measured the complex broadband microwave conductivity of Si:P from 100 MHz to 5 GHz in a broad range of phosphorus concentration $n = n_c$ from 0.56 to 0.95 relative to the critical value $n_c = 3.5 \cdot 10^{18} \text{ cm}^{-3}$ corresponding to the metal-insulator transition driven by doping.

At our base temperature of $T = 1.1 \text{ K}$ the samples are in the zero-phonon regime where they show a super-linear frequency dependence of the conductivity indicating the influence of the Coulomb gap in the density of the impurity states. At higher doping $n > n_c$, an abrupt drop in the conductivity power law $\sigma_1(\omega) \propto \omega^{-1}$ is observed. The dielectric function ϵ_1 increases upon doping following a power law in $(1 - n/n_c)$. Dynamic response at elevated temperatures has also been investigated.

Copyright line will be provided by the publisher

1 Introduction In a material of such an industrial importance like Si:P there are still questions open about the low-energy excitations from the ground state. In particular, the influence of electron-electron interactions on the hopping transport and the critical behavior at the metal-insulator transition (MIT) have attracted much attention since decades. Though theoretical predictions on the $T \rightarrow 0$ frequency-dependent response of an interacting disordered system have already existed since many years [1], experimental data still remain scarce and results obtained by different groups and in different parameter ranges lack consistency. Especially in the microwave range, from tens of MHz till tens of GHz, with wavelengths from a few millimeters to a few meters, no better means than the resonator techniques have been used for a long time to study the broadband dynamic conductivity of doped semiconductors. With a novel and advanced method of measuring the broadband (100 MHz to 5 GHz) complex microwave conductivity of that material class, we focus on the conductivity power law in Si:P at $T \rightarrow 0$ and at elevated temperatures in a broad range of donor concentration close to

the MIT.

At concentrations of phosphorus in silicon below the critical value of $n_c = 3.5 \cdot 10^{18} \text{ cm}^{-3}$, the donor electron states are strongly localized due to disorder in Anderson sense [2] and the corresponding wave functions resemble those of a hydrogen atom [3]. Since some degree of compensation by impurities of the opposite type is considered inevitable, charge transport at low excitation energies is by variable-range hopping between the donor sites, randomly distributed in space [3,4].

1.1 Dynamic conductivity The static conductivity σ_{dc} of the insulating Si:P vanishes when $T \rightarrow 0$. The main issue we address is that of power laws of the frequency-dependent conductivity in the variable-range hopping regime at zero temperature:

$$\sigma_1(\omega) \propto \omega^{-1}; \quad \epsilon_1 = \epsilon_1 + i\epsilon_2 \quad (1)$$

The theory of resonant photon absorption by pairs of states, one of which is occupied by an electron and the other one

Copyright line will be provided by the publisher

is empty, yields distinct limiting results for the conductivity power law in cases, where one of the relevant energy scales of the problem dominates over the others:

For the non-interacting system, where the photon energy prevails over the electronic correlations, Mott has predicted a sub-quadratic frequency-dependence of the conductivity [4]:

$$\begin{aligned} \sigma_1(\omega) &= \epsilon^2 g^2 a r_1^4 \omega^{-2}; \\ r_1 &= a \ln(2I_0/\omega); \end{aligned} \quad (2)$$

Here, ϵ is a numerical coefficient [1,4], g is the state density at the Fermi level, a is the localization radius, r_1 is the most probable hopping distance and I_0 is the pre-exponential factor of the overlap integral between the localized electron states.

Taking into account the Coulomb repulsion $U(r_1)$ if both states in a pair would be occupied by an electron, Shklovskii and Efros corrected the picture of the energy levels before and after a photon is absorbed and derived $\sigma_1(\omega)$ to be a sub-linear function of frequency, as long as the Coulomb interaction term dominates over the photon energy [1]:

$$\begin{aligned} \sigma_1(\omega) &= \epsilon^2 g^2 a r_1^4 \omega^{-1} [1 + U(r_1)]; \\ U(r_1) &= \frac{e^2}{\epsilon_1 r_1}; \end{aligned} \quad (3)$$

At higher frequencies, in the opposite limit, the sub-quadratic behavior known from Mott (2) is recovered.

The formula (3) is derived under the assumption of an effectively constant density of states g near the Fermi level. This implies another characteristic energy of the system, the Coulomb gap ϵ , to be small compared to $U(r_1)$ and thus of no significant effect on the states participating in the hopping transport. The parabolic Coulomb gap forms in the density of the impurity states around the Fermi level as another consequence of the electronic correlations [3]. For the conductivity of interacting electrons where the Coulomb term $U(r_1)$ dominates over the photon energy but falls inside the Coulomb gap, the reduction of the density of states leads to a stronger, slightly super-linear power law [1]:

$$\sigma_1(\omega) \propto \omega^{-1} \ln(2I_0/\omega); \quad (4)$$

1.2 Dielectric function It is an additional advantage of a phase sensitive measurement to gain the dielectric function ϵ_1 from the imaginary part of the complex conductivity $\sigma = \sigma_1 + i\sigma_2$ [5]:

$$\epsilon = \epsilon_1 + i\epsilon_2 = 1 + i \frac{\sigma}{\omega \epsilon_0}; \quad (5)$$

We denote by ϵ the full complex dielectric function of Si:P, relative to the permittivity ϵ_0 of vacuum, and use the SI units throughout this text. As the MIT is approached upon doping n , the localization radius a diverges according to a power law [3]:

$$a \propto |n - n_c|^{-1};$$

As a consequence, the electronic contribution to the dielectric function is also expected to diverge following a power law when the MIT is approached [6]:

$$\epsilon_1 \propto |n - n_c|^{-2}; \quad (6)$$

where $\epsilon_{Si} = 11.7$ is the dielectric constant of the host material Si.

2 Experiments

2.1 Samples

Si:P-samples for this study were cut from a Czochralski-grown cylindrical crystal [7], nominally uncompensated, with a phosphorus concentration gradient along its axis. To remove distorted surface layers [8, 9], the samples were chemically and mechanically treated by well established procedures. The donor concentration was determined from the room-temperature resistivity [10] employing a commercial four-probe measurement system (FPP 5000 by Veeco Instruments). For high doping levels the resistivity ratio $\rho(4.2K)/\rho(300K)$ (determined from standard dc measurements) is consistent with Ref. [11]. In the present work, measurements on Si:P-samples with relative donor concentration n/n_c ranging from 0.56 to 0.90 relative to the critical value at the MIT are discussed, as summarized in Tab. 1.

Table 1 Dopant concentration n and the value of the room-temperature dc resistivity ρ_{dc} of the presented Si:P-samples. The second column lists the relative concentration with respect to the critical value $n_c = 3.5 \cdot 10^{18} \text{ cm}^{-3}$ at the MIT. The power α of the conductivity power law $\sigma_1(\omega) \propto \omega^{-\alpha}$ and the full relative dielectric constant ϵ_1 are also displayed in Fig.4 and Fig.7

n (10^{18} cm^{-3})	n/n_c	ρ_{dc} (300 K) ($\Omega \text{ cm}$)	α	ϵ_1
1.97	0.56	0.0162	1.13	23
2.29	0.65	0.0149	1.16	24.5
2.57	0.73	0.0139	1.10	28
2.91	0.83	0.0130	1.08	34
3.04	0.87	0.0127	1.05	41
3.14	0.90	0.0124	1.04	46

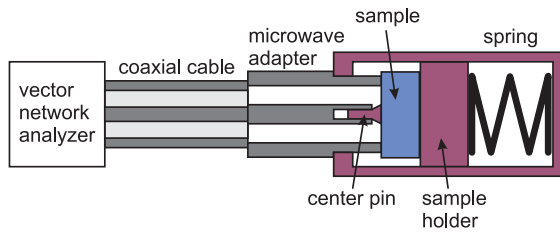


Figure 1 Schematic of a broadband microwave spectrometer that employs a vector network analyzer. A solid sample terminates the otherwise open-ended coaxial line (after [13]).

2.2 Broadband microwave spectroscopy

The broadband microwave spectrometer, previously employed for measuring metallic samples [13, 14], has been upgraded [12] with microwave components, calibration technique and evaluation procedure suitable to study the hopping transport in doped semiconductors at temperature as low as possible.

The sample with a flat surface terminates the 1.2m-long coaxial line, Fig.1, needed to transport the microwave signal from the source to the bottom of a ⁴He-pumped cryostat. The reflected signal, containing all the useful information about the sample, returns the same way back to the test set of a HP 8510 vector network analyzer. The measurement is phase sensitive and yields the complex reflection coefficient. After an extensive calibration procedure requiring three independent low temperature measurements of calibration samples under reproduced conditions, the reflection coefficient S_{11} at the sample surface is obtained. The complex impedance Z is directly related to it via [15]:

$$S_{11} = \frac{Z - Z_0}{Z + Z_0} ; \quad (7)$$

with the characteristic impedance Z_0 of the microwave line.

In a next step, the complex conductivity σ has to be extracted from the impedance Z . If material is insulating, there exists no direct solution, because the simple concepts known from metallic samples [14] fail here. In the case of an insulator, the surface impedance approach [5], useful for thick metallic samples, yields a wrong (i.e. too strong) frequency dependence of the conductivity σ_1 . If the semi-conducting sample is treated as a thin highly-conducting film, the conductivity values are suspiciously large [16].

2.3 Advanced data analysis

For these reasons, we have developed a general and rigorous solution for the problem. The electromagnetic wave penetrates deep into a thick insulating sample, Fig.2, and forms a three-dimensional distribution quite different from that of a plane wave. Thus, we work with a solution for the field distribution in an integral equation formulation, combined with the variational principle [17]. Ascertaining, that the electromagnetic field strength decreases below 1% at the depth corresponding to our sample thickness of 2 mm in the frequency range evaluated, we forbear from taking into account the secondary reflections at the back side of the sample as in the full-

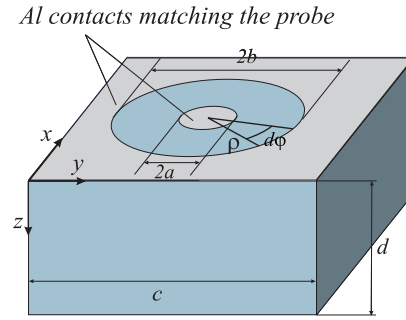


Figure 2 Sketch of the Si:P-sample with the aluminium contact-layer on top. $2a = 0.6$ mm, $2b = 1.75$ mm, corresponding to a 2.4 mm microwave adapter, $c = 5$ mm, $d = 2$ mm

wave analysis at higher frequencies considered by Brom and collaborators [18]. The resulting formula connects the complex sample impedance Z to the wave vector k , the latter containing the complex dielectric function ϵ we search for. (Note, that we hold to the convention $\exp(i(k \cdot x - \omega t))$ for the Fourier-transformed of the electromagnetic field in accordance with [5, 17]. The opposite sign convention is used in Ref. [18, 19] and by the network analyzer.)

$$\frac{Z_0}{Z} = \frac{ik^2}{k_c \ln(b/a)} \int_0^{2b} \int_0^{2a} \cos' \frac{\exp(ikr)}{r} d' d d d^0 ; \quad (8)$$

$$r = (\rho^2 + z^2)^{1/2} ;$$

To solve this integral equation for k we make use of the practical ideas from [19]. In a series expansion of the exponential function the terms higher than the third term are negligible below 5 GHz, integrating the rest one obtains a quadratic equation in $\epsilon = \epsilon_1 + i\epsilon_2$ [12]:

$$\frac{1}{Z} = \frac{i2! \epsilon_0''}{[\ln(b/a)]^2} I_1 - \frac{!^2 \epsilon_0 I_3''}{2} \quad (9)$$

with the geometrical integrals $I_1 = 0.9084$ mm and $I_3 = 0.2100$ mm³ numerically evaluated for the dimensions a and b of our coaxial probe as shown in Fig.2.

2.4 Low-temperature ac measurements

The frequency range from 100 MHz to 5 GHz for the reflection coefficient measurements according to section 2.2 contains 300 frequency points: 200 equidistant points from 0.1 GHz to 1 GHz and 100 from 1 GHz to 5 GHz. The spectra are taken at the base temperature 1.1 K of our ⁴He-pumped cryostat as well as at elevated temperatures using a temperature controller Lake Shore 340 in an automatized procedure while heating the setup up to room temperature. All the reported samples prove to be in the zero-phonon regime at $T = 1 \pm 1$ K because they show a saturation of $\sigma_1(T)$ and $\epsilon_1(T)$ in the whole frequency range as $T \rightarrow 1$ K.

3 Results and discussion

For each doping concentration n four to ten independent measurements have been

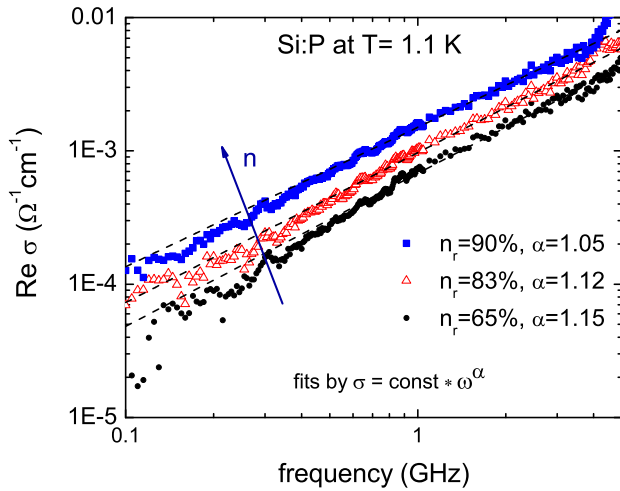


Figure 3 Typical spectra of the measured real part of the conductivity for Si:P with relative donor concentrations $n=n_c$ of 0.65, 0.83 and 0.90. The dashed lines are the fits by a two-parameter power law function.

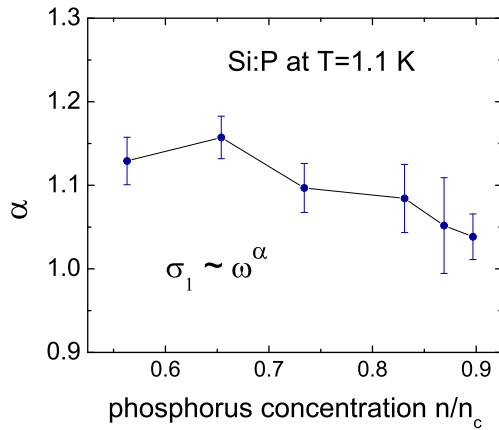


Figure 4 Mean value of the conductivity power α obtained from the $\sigma_1 \sim \omega^\alpha$ fit. The dependence on the relative donor concentration $n=n_c$ becomes stronger as $n \rightarrow n_c = 3.5 \cdot 10^{18} \text{ cm}^{-3}$.

conducted. From the best spectra (lowest noise and smallest influence of standing waves) mean values of the conductivity power α and the dielectric constant ϵ_1 have been determined.

3.1 Frequency dependence of the conductivity in the zero-phonon regime In Fig.3 the measured real part of the frequency-dependent conductivity is plotted on a log-log scale to identify the power law. The fits by a two-parameter function $\sigma_1(\omega) = \text{const} \cdot \omega^\alpha$ crossing the origin are shown by the dashed lines. In Fig.4 the mean values of the power α are plotted against the relative dopant concentration. The frequency dependence of the conductivity clearly follows a super-linear power law in the whole do-

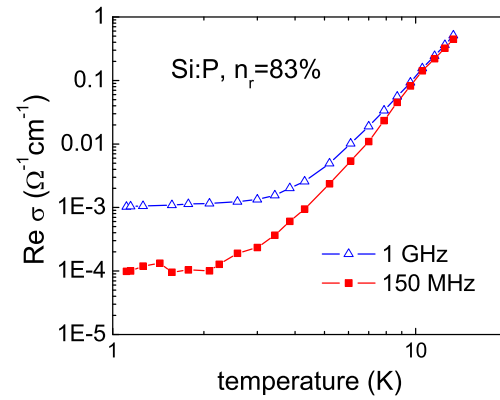


Figure 5 Temperature dependence of the conductivity at fixed frequency on example of relative doping $n=n_c = 0.83$, typical for all the investigated Si:P-samples.

ping range, where the exponent decreases slightly with doping; this effect becomes even stronger when n is increased further. From this we infer, that hopping transport takes place deep inside the Coulomb gap corresponding to equation (4). A super-linear conductivity power law was previously observed in Si:As and Si:P by Castner and collaborators [20,21] using resonator techniques at certain frequency within the range of the present work. Our results are in accord with the measurements on similar samples at higher frequencies (30 GHz to 3 THz) using optical techniques [22,23]. In contrast, a sub-linear frequency dependence in the zero-phonon regime has been reported by Lee and Stutzmann [16] based on experiments on Si:B in the microwave range and by Helgren et al. [9] using quasi-optical experiments.

3.2 Temperature dependence of the conductivity

Leaving the zero-phonon regime by raising temperature, a gradual increase of the conductivity σ_1 is observed for all investigated Si:P-samples. First, the temperature dependence is approximately linear in agreement with the prediction of Austin and Mott [1,24]. With increasing T , it gradually becomes stronger until the charge carrier activation into the conduction band dominates over the hopping transport. The onset of the thermal effects depends on the phosphorus concentration: the higher the doping, the lower the temperature at which the temperature dependence sets in. But the way it happens is the same for all the samples measured. Taking the example of $n=n_c = 0.83$, we have plotted the conductivity values in Fig.5 at fixed frequencies of 150 MHz and 1 GHz. Above $T = 9 \text{ K}$ the curves merge into the thermally activated curve.

In fig. 6 the frequency dependent conductivity is plotted for different temperatures, for the example of the crystal with the high concentration $n=n_c = 0.9$; the conductivity power law gradually decreases with rising temperature. The transition to a sub-linear power law upon raising T is in accord with previous observations [21,24,25]; to

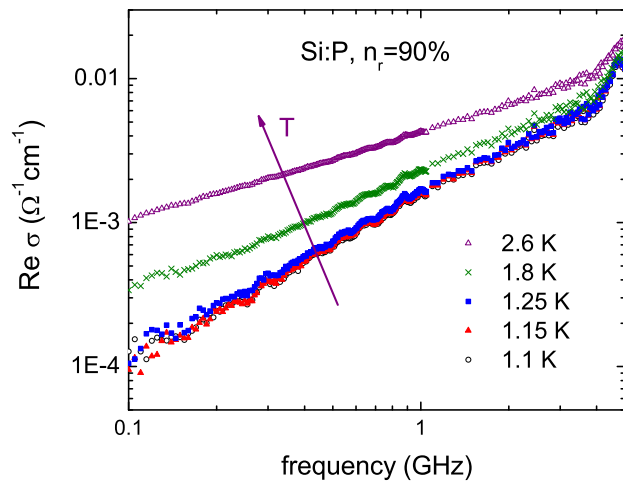


Figure 6 Temperature dependence of the conductivity spectra typical for all the investigated Si:P-samples.

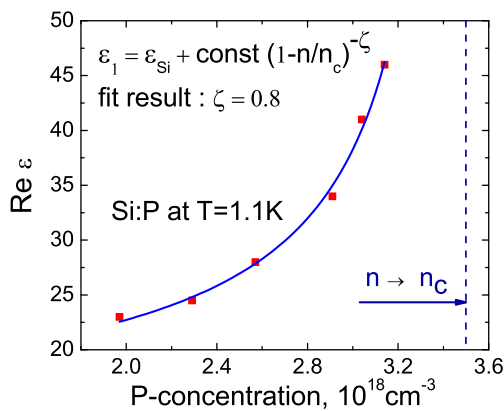


Figure 7 Doping dependence of the low-temperature dielectric constant of Si:P. The solid line is the fit with the power law function (6) for the electronic dielectric function $\epsilon_1 = \epsilon_{Si} + \text{const} (1 - n/n_c)^{-\zeta}$.

our knowledge, the theoretical description of the gradual decrease of ϵ_1 is lacking.

3.3 Dielectric function The dielectric function ϵ_1 is independent of frequency in our frequency range, taking the measurement uncertainty into account. A fit with the function (6) results in an exponent $\zeta = 0.8$, as shown in Fig.7.

4 Conclusion Si:P-samples with relative doping $n = n_c$ from 56% to 90% show temperature-independent dynamic response at the temperature of 1.1 K. Over a wide frequency range (100 MHz to 5 GHz) the conductivity power law is slightly super-linear, with a faint decrease of the power upon doping. At higher doping, above 90 %, the conductivity power law drops abruptly. Interpretation and further studies at lower base temperature using ^3He are in

progress. At elevated temperatures the conductivity values are increasing and the power is falling gradually with rising T . The electronic contribution to the dielectric function is constant and increases with phosphorus concentration as expected when the MIT is approached.

Acknowledgements We thank A. L. Efros, H. v. Löhneysen and K. Holczer for helpful discussions, A.W. Anajoh and M. Scheffler for the dc-measurements and die Landesgraduiertenförderung Baden-Württemberg for the scholarship.

References

- [1] B. I. Shklovskii and A. L. Efros, Zh. Eksp. Teor. Fiz. **81**, 406 (1981) [Sov. Phys. JETP **54**, 218 (1981)]
- [2] P. W. Anderson, Phys. Rev. **109**, 1492 (1958)
- [3] B. I. Shklovskii and A. L. Efros, Electronic Properties of Doped Semiconductors (Springer, Berlin, 1984),
- [4] N. F. Mott and E. A. Davis, Electronic Processes in Non-Crystalline Materials, 2nd edition (Clarendon Press, Oxford, 1979),
- [5] M. Dressel and G. Grüner, Electrodynamics of Solids (Cambridge University Press, Cambridge, 2002)
- [6] A. L. Efros and B. I. Shklovskii, phys. stat. sol. (b) **76**, 475 (1976)
- [7] Single crystal grown by Société Générale Métallurgique de Hoboken and provided by D. Schweitzer.
- [8] Y. Ootuka, F. Komori, Y. Monden, S. Kobayashi, and W. Sasaki, Solid State Commun. **36**, 827 (1980)
- [9] E. Helgren, N. P. Armitage, and G. Grüner, Phys. Rev. B **69**, 014201 (2004)
- [10] W. R. Thurber, R. L. Mattis, Y. M. Liu, and J. J. Filliben, J. Electrochem. Soc. **127**, 1807 (1980)
- [11] M. Hornung, Diploma thesis, Karlsruhe (1993)
- [12] E. Ritz and M. Dressel, to be published
- [13] M. Scheffler and M. Dressel, Rev. Sci. Instrum. **76**, 074702 (2005)
- [14] J. C. Booth, Dong Ho Wu, and S. M. Anlage, Rev. Sci. Instrum. **65**, 2082 (1994)
- [15] D. M. Pozar, Microwave Engineering (John Wiley & Sons, New York, 1998)
- [16] M. Lee and M. L. Stutzmann, Phys. Rev. Lett. **87**, 056402 (2001)
- [17] H. Levine and C. H. Papas, J. Appl. Phys. **22**, 29 (1951)
- [18] H. C. F. Martens, J. A. Reedijk, and H. B. Brom, Rev. Sci. Instrum. **71**, 473 (2000)
- [19] D. K. Misra, IEEE Trans. Microwave Theory Tech. **MTT-35**, 925 (1987)
- [20] R. J. Deri and T. G. Castner, Phys. Rev. Lett. **57**, 134 (1986)
- [21] M. Migliuolo and T. G. Castner, Phys. Rev. B **38**, 11593 (1988)
- [22] M. Hering, M. Scheffler, M. Dressel, and H. v. Löhneysen, Physica B **359**, 1469 (2005)
- [23] M. Hering, M. Scheffler, M. Dressel and H. v. Löhneysen, Phys. Rev. B **75**, 205203 (2007)
- [24] I. G. Austin and N. F. Mott, Adv. Phys. **18**, 41 (1969)
- [25] M. Pollak and T. H. Geballe, Phys. Rev. **122**, 1742 (1961)